

Modification of growth kinetics in surfactant-mediated epitaxy

Bert Voigtländer, Andre Zinner, Thomas Weber, and Hans P. Bonzel

Institut für Grenzflächenforschung und Vakuumphysik, Forschungszentrum Jülich, 52425 Jülich, Germany

(Received 24 October 1994)

The influence of Sb, As, Ga, and In as surfactants on the Si/Si(111) homoepitaxy is studied using scanning tunneling microscopy. The nucleation of two-dimensional (2D) Si islands on the surfactant-terminated surface was studied as a function of temperature. The island densities and depleted zones show Arrhenius behavior. Surfactants modify the Si epitaxy in quite a different way. Indium as surfactant increases the diffusivity of the Si atoms, whereas Sb and As drastically decrease the diffusion length of Si. When we apply these results to Ge epitaxy on Si the reduction of the diffusion length is shown to be essential for the suppression of 3D islanding in surfactant-mediated Ge/Si heteroepitaxy. Generally, elements of group III and IV as surfactants that enhance the diffusivity in Si homoepitaxy lead to 3D islanding in Ge/Si heteroepitaxy. Elements of group V and VI reduce the diffusion length in Si homoepitaxy and give rise to a suppression of 3D islanding in Ge/Si heteroepitaxy. The temperature dependence and rate dependence of the nucleation of 2D islands in Si/Si(111) homoepitaxy can be described in the framework of classical nucleation theories yielding a critical nucleus size of 6 and an activation energy of diffusion of 0.75 eV. Experimentally no indication for a reflective potential barrier for step-down motion of diffusing Si atoms (Ehrlich-Schwoebel barrier) was found.

INTRODUCTION

Recently, the use of additional surface species (surfactants) which modify the epitaxial growth has attracted a lot of interest.¹⁻⁴ In surfactant-mediated epitaxy a monolayer of surfactant material, which floats at the growth front influences the epitaxial growth. Especially it has been shown that the normally occurring three-dimensional (3D) islanding of Ge on Si (Stranski-Krastanov growth) can be suppressed by the use of suitable surfactants.¹⁻⁴

This method of surfactant-mediated growth is currently used in device oriented research to improve the quality of strained Si/Ge superlattices.^{5,6} Additionally flat, relaxed Ge layers on silicon substrates which can be grown with surfactant-mediated epitaxy⁴ could be used to improve the quality of Ge buffer layers, which are often used in GaAs epitaxy on Si. While surfactants are already used to improve the quality of Ge layers on Si the question why certain surfactants suppress 3D islanding in Ge/Si heteroepitaxy while others do not is not yet answered. One necessary requirement for a surfactant to work is the floating of the surfactant during growth. The reduction of surface free energy is the driving force for the surfactant to float during growth. However, this modification of the surface free energy alone is not sufficient to suppress 3D islanding. For instance, Pb floats during Ge growth on Si but leads to 3D islanding in an early stage of growth.⁷

Besides the fact that the surfactants influence the energies during growth (by lowering the surface free energy), they can also influence drastically the kinetics during growth.⁸ In this paper, we focus on the modification of growth kinetics by surfactants. If the Si adatoms would diffuse rapidly on the surfactant passivated surface, enhanced diffusion would lead to a step-flow growth

mode. If, on the other hand, arriving atoms are incorporated rapidly below the surfactant layer, the diffusion is drastically curtailed. The study of the nucleation of 2D islands during submonolayer epitaxy by scanning-tunneling microscopy (STM) can determine the island density and diffusion length as a function of temperature and rate. Scanning-tunneling-microscopy measurements can provide a direct access to the growth kinetics and reveal the mechanisms in surfactant-mediated epitaxy. Here, in particular, homoepitaxy offer the opportunity to study solely the influence of surfactants on growth, while other effects like strain which influence growth in heteroepitaxy are not present.

We find that In enhances the diffusivity of Si, while Sb and As are shown to drastically reduce the Si diffusion length. If we carry over the results from Si homoepitaxy to the Ge growth on Si, the reduction of the Ge diffusion length in surfactant-mediated epitaxy is shown to be a mechanism for the suppression of three-dimensional islanding in Ge/Si heteroepitaxy. More generally elements of group III and IV as surfactants enhance the diffusivity in Si homoepitaxy and lead to 3D islanding in Ge/Si heteroepitaxy. Elements of group V and VI reduce the diffusion length in Si homoepitaxy which leads to a suppression of 3D islanding in Ge/Si heteroepitaxy.

EXPERIMENT

The STM measurements were performed in an ultrahigh vacuum chamber (base pressure $< 10^{-10}$ mbar). The Si(111)7×7 substrates ($\approx 1 \times 10^{19}$ Sb atoms/cm³ doping) were prepared by degassing for 12 h at 600 °C and short flash to 1200 °C. The STM images were taken in the constant current mode at sample bias voltages between 2.7 and -2.7 V and a tunneling current between 0.1–1 nA.

Si was grown using an electron-beam evaporator equipped with electrostatic plates to deflect Si ions from the sample. Si was evaporated at a rate of 0.2 ML/min (1 ML = 7.8×10^{14} atoms/cm²). A quartz-crystal balance and the STM images were used to measure the deposited Si amount. Sb was evaporated on the silicon at a sample temperature of 670 °C to terminate the surface by 1-ML Sb [$(\sqrt{3} \times \sqrt{3})R 30^\circ$ LEED structure]. An effusion cell was used to evaporate As. During As evaporation the sample was held at 700 °C. After the furnace was shut off the sample temperature was lowered to 500 °C until the pressure was below 10^{-9} mbar. Then the sample was cooled to room temperature. A sharp (1×1) LEED pattern was observed indicative of a 1-ML As-terminated surface.⁹ Using Ga as a surfactant $\frac{1}{3}$ -ML Ga was evaporated with the sample held at 650 °C. Scanning-tunneling-microscopy images of this surface show that the Si(111) terraces are covered by a $(\sqrt{3} \times \sqrt{3})R 30^\circ$ structure. The In terminated surface was prepared by evaporating $\frac{1}{3}$ ML of In at 580 °C. This resulted in broad terraces of a $(\sqrt{3} \times \sqrt{3})R 30^\circ$ In structure.

GROWTH OF Si ON Si(111)

Before we turn to the influence of surfactants, we study the Si/Si homoepitaxy as a reference. Silicon homoepitaxy proceeds in nucleation, growth, and coalescence of 2D islands. Here, we focus on the rate and temperature dependence of the density of 2D islands, which grow during submonolayer Si evaporation. In the framework of classical nucleation theories, quantities such as the diffusion energy of Si on Si(111) and the number of Si atoms that form a stable cluster can be determined.

Nucleation of new islands and growth of existing islands are competing processes. The contribution of both processes is determined by the diffusion length, on the one hand, and the number of atoms and the energy to form stable nuclei, on the other hand.^{10,11} The dependence of the island density on the diffusion can be rationalized as follows: Arriving atoms from the vapor provide a certain adatom density on the surface. When a critical value of the adatom density is reached, stable nuclei are formed which grow to 2D islands. Around an existing island the adatom density is reduced by adatom diffusion to and incorporation in an existing island. No further stable nuclei can form in a zone around existing islands. If we take the mean distance between islands as a characteristic length for the diffusion, this length R is related to the island density N by $R = 1/\sqrt{N}$. When the diffusivity is increased (e.g., by increasing the temperature), the characteristic length for diffusion will increase and correspondingly the island density will decrease. Another length characteristic for the diffusion is the width of the depleted zone at step edges, which is analogous to the mean distance between islands. The process competing with diffusion, the nucleation of new islands, is described by a critical nucleus size i and a binding energy $E_c(i)$.¹¹ Clusters with a size up to the critical size can grow and decay by attachment and detachment of diffusing atoms, respectively. If the cluster has grown to a certain critical size i , attachment of further atoms forms a stable cluster

($n > i$), which cannot decay. Additionally, the nucleation depends on the binding energy $E_c(i)$ to form a critical cluster from i single adatoms.

Figure 1(a) shows an area of about $0.6 \times 0.6 \mu\text{m}$ of the Si(111) surface. The three terraces visible in this region are separated by 3.2-Å-high steps. About 15% of a Si(111) double layer was evaporated at 500 °C. Triangular 2D islands nucleate on the terraces. Apart from homogeneous nucleation on the terraces, preferred nucleation occurs at the (7×7) domain boundaries [rows of islands in the upper right and lower left of Fig. 1(a)]. The scan range of this image is too large to resolve the (7×7) reconstruction present on the terrace. Zones depleted from islands are observed near step edges. These results agree with previous measurements.¹²

Figure 1(b) shows that, at a higher growth temperature (550 °C), the island density decreases and the depleted

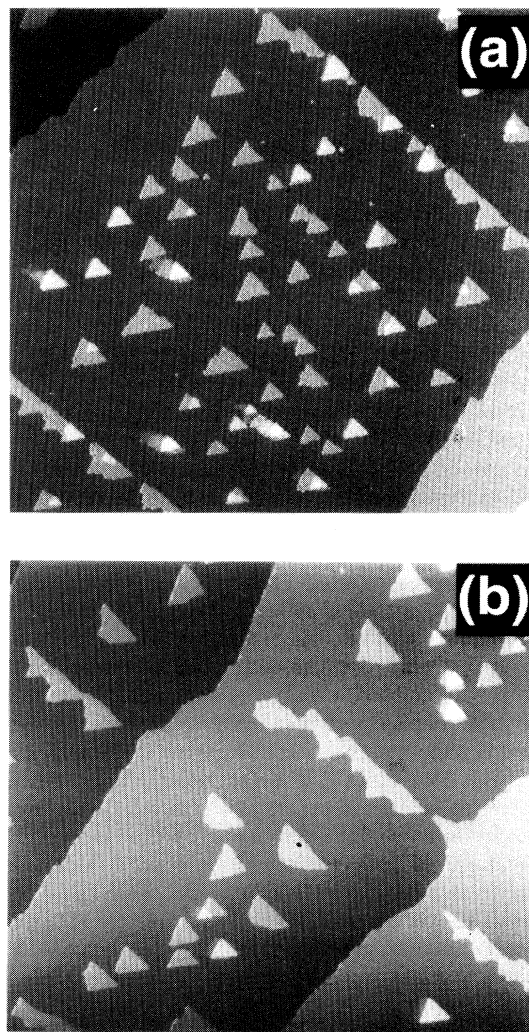


FIG. 1. Scanning-tunneling-microscopy images of 2D Si islands on a Si(111) terrace. Preferred nucleation occurs at (7×7) domain boundaries and depleted zones exist near step edges. (a) Area: $5800 \times 5800 \text{ \AA}$, $T = 500^\circ\text{C}$. (b) Epitaxy at higher temperature results in wider depleted zones and smaller island densities (area: $9100 \times 8600 \text{ \AA}$, $T = 550^\circ\text{C}$).

zone at the step edges widens due to the increased diffusion at higher temperatures. The temperature-dependent island density shows an Arrhenius behavior [Fig. 2(a)]. Apart from the temperature, the growth kinetics is also influenced by the evaporation rate of the incoming silicon. At a higher evaporation rate nucleation events become more probable. More Si atoms diffusing on the surface lead to more nucleation events and hence to higher island densities and smaller depleted zones. Figure 2(b) shows that a power-law behavior is observed for the island density as function of the rate.

For further quantitative analysis we used the nucleation theory of Venables, Spiller, and Hanbücken,¹¹ where rate equations describing the nucleation and growth are used to derive an equation for the island density. In the regime of complete condensation (no reevaporation to the vacuum), the island density (N) can be expressed as

$$N \sim \left(\frac{R}{\nu} \right)^{i/(i+2)} \exp \left[\frac{E_c(i, E_b) + iE_d}{kT} \right]^{1/(i+2)}. \quad (1)$$

The first term of Eq. (1) describes the rate dependence of the island density. The second term which will be dis-

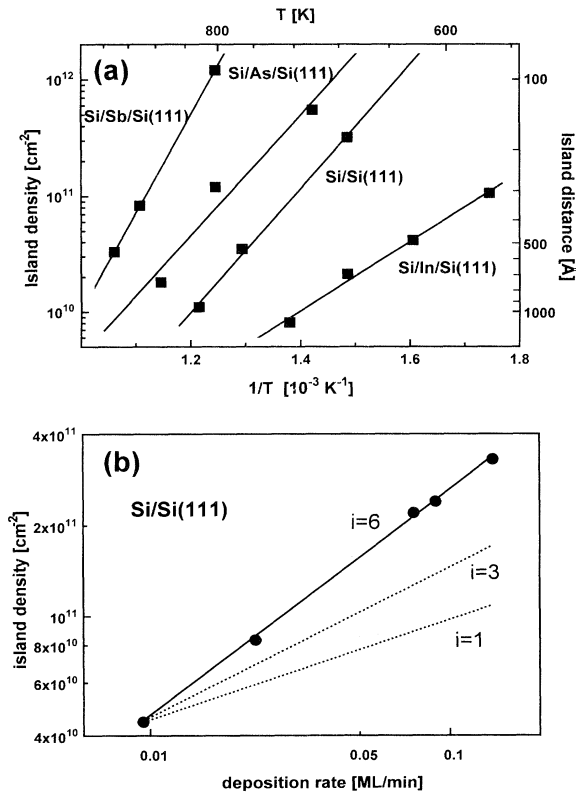


FIG. 2. (a) Island density for submonolayer Si coverage shows Arrhenius behavior. Island densities higher than in pure Si homoepitaxy (Sb,As) indicate small diffusion length and low island densities (In) indicate high diffusivity. (b) Island density in Si/Si epitaxy as function of rate ($T=410^\circ\text{C}$). A power-law behavior with a slope of 0.85 is observed. From classical nucleation theories the size of the critical nucleus ($i=6$) and a diffusion energy of 0.75 eV can be determined.

cussed below describes the temperature dependence of N (ν is the atomic vibration frequency $\approx 10^{12}$ Hz). The dependence of the island density as function of the rate (R) is a power law as observed experimentally [Fig. 2(b)]. From the exponent the critical nucleus size i can be determined to 6. The dashed lines in Fig. 2(b) are drawn for $i=1, 3$, and 6. This means that very small critical clusters, e.g., with $i=1$ as proposed for Si/Si(100) epitaxy¹⁰ are excluded on Si(111). Critical cluster sizes between 5 and 8 are compatible with the experiment. This is reasonable because on Si(111) a bilayer of silicon is formed during growth requiring larger critical nuclei than for single-layer growth. With the critical nucleus size known from the rate dependence, the diffusion energy (E_d) can be estimated from the temperature dependence of the island density [second term in Eq. (1)]. $E_c(E_b, i)$ is the binding energy that is gained when i single adatoms form a cluster of the size i . E_b is the energy of a single Si-Si bond (~ 1.7 eV).¹³ In the simplest model E_c is just E_b times the number of bonds gained by forming a cluster from i adatoms. The formation energy of the critical nucleus influences the island density in the following way: With increasing energy (E_c) cluster formation becomes energetically more favorable and the island density increases. For the activation energy of diffusion we obtain $E_d=0.75$ eV. The largest uncertainty in the determination of E_d is the assumption $E_b \sim 1.7$ eV. An independent estimate of the binding energy from the sublimation energy¹⁴ results in $E_b < 2.3$ eV. An error in E_b of 0.5 eV corresponds to 0.2-eV error for E_d . So we obtain $E_d=0.75 \pm 0.2$ eV.

When we analyze the depleted zones at both sides of a step edge, we find a wider depleted zone at the upper side of the step than at the lower side [Fig. 1(a)]. This asymmetry can be explained simply by the diffusion of adatoms to the steps on both sides of the terraces, upper and lower. The incorporation of these adatoms at the step leads to a motion of the step towards the lower terrace. This causes an asymmetry in the depleted zones. For a known Si coverage (from the images) the asymmetry of the depleted zones can be estimated quantitatively and compared to the measured values. All of the observed asymmetry can be explained by the effect of step motion with coverage.

Recently, a reflective potential barrier (Ehrlich-Schwoebel barrier) for step-down diffusion was discussed in metal on metal epitaxy.¹⁵⁻¹⁷ Such a barrier should also lead to an asymmetry in the depleted zones at the step edges. However, in this case, the asymmetry should have the opposite direction than for pure step motion. Si atoms are deposited isotropically and diffuse on the surface. If they are reflected at the upper step edges due to a potential barrier for a jump in step-down direction, this would lead to an increased adatom density at the upper step edges and hence to an increased nucleation probability. This would result in a smaller denuded zone at the upper side of the step.

Based on such a comparison of island-free zones on the upper and lower terrace near a step, we find no indication for a reflective potential barrier for the adatom motion in step-down direction. This means that the height of a pos-

sible barrier is smaller than kT . So the interlayer mass transport which is promoted by surfactant-mediated growth in metal epitaxy¹⁶ is already possible in silicon epitaxy without surfactant. The use of surfactants in Ge/Si heteroepitaxy is to suppress the thermodynamically stable 3D-island growth.

Sb AND As AS SURFACTANTS

Using the results of the pure Si homoepitaxy as a reference, we studied the modification of growth kinetics and morphology by different surfactants. First the Si(111) surface was terminated with 1-ML Sb prior to the Si growth. The Si surface exhibits a $(\sqrt{3}\times\sqrt{3})R30^\circ$ Sb reconstruction, which consists of Sb trimers on top of a complete Si(111) bilayer.¹⁸ Figure 3(a) shows a STM image of 975×620 Å after a submonolayer deposition of Si. The island density increases drastically in the Sb mediated growth. At 530°C the island density is 100 times larger than in pure Si/Si(111) homoepitaxy. This increased island density can be explained by a drastically reduced diffusion length in Sb-mediated epitaxy. The alternative explanation that the higher island density can be explained by nucleation at defects in the Sb overlayer

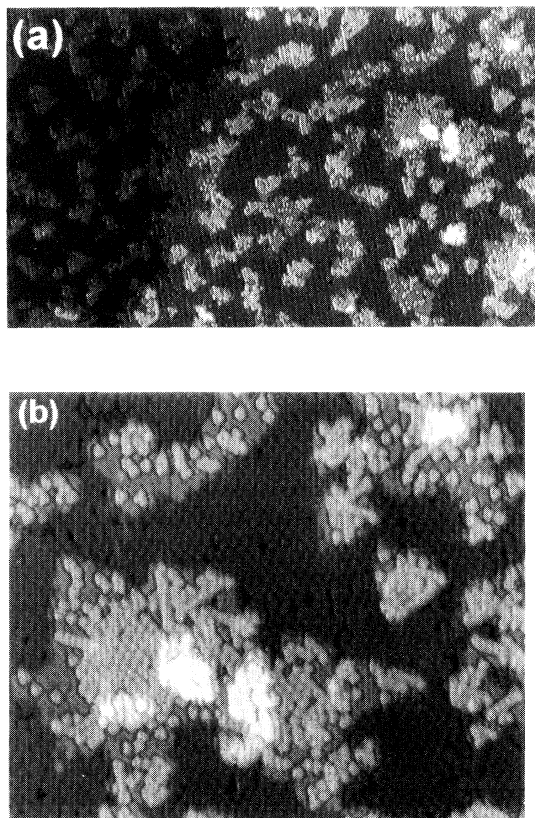


FIG. 3. Antimony-mediated epitaxy of Si on Si(111) ($T=530^\circ\text{C}$) increases the island density drastically and reduces diffusion length. (a) Area: 975×620 Å; (b) higher-resolution scan of upper right in (a), area: 325×290 Å. The surface is completely covered by Sb. On the silicon terrace and on top of the 2D islands a $(\sqrt{3}\times\sqrt{3})$ -Sb structure is observed. The flat areas at the edges of the islands are Sb(1 \times 1).

can be excluded. Temperature-dependent measurements show an Arrhenius behavior [Fig. 2(a)]. Such a temperature dependence is not expected for nucleation at defects. We prepared the starting surface at higher temperature (670°C) than the temperature used during Si evaporation. So the defect density in the $(\sqrt{3}\times\sqrt{3})R30^\circ$ Sb layer was the same in all experiments and the Arrhenius behavior can only be explained by the temperature dependence of the diffusion length.

The reduced diffusion length in the Sb-mediated Si epitaxy is also shown by other characteristic features of the growth morphology: The island shape and the form of the steps are irregular compared to the triangular island shape and the straight steps in pure Si/Si homoepitaxy. The atomic structure resolved in Fig. 3(b) shows that the surface is Sb terminated. We do not find the (7 \times 7) reconstruction typical for pure Si(111) but on the terrace between the 2D islands, we observe the $(\sqrt{3}\times\sqrt{3})R30^\circ$ structure of Sb trimers typical for the Sb terminated Si(111) surface.¹⁸ On top of the 2D islands, we find three different types of atomic structure which can also be attributed to a Sb-terminated structure. Apart from areas of $(\sqrt{3}\times\sqrt{3})R30^\circ$ structure, we find areas of (1 \times 1) structure which can be explained by Sb incorporated into the upper half of the Si bilayer and occasionally areas with a (2 \times 1) zigzag structure.³ The (1 \times 1) and (2 \times 1) Sb structures were also previously observed on a Sb terminated Ge(111) surface.³ By assigning all of the observed atomic structures to a Sb-terminated surface, we conclude that the island surface is completely Sb terminated. The Sb(1 \times 1) structure occurs preferentially at the step edges of the 2D islands. This shows that the surfactant-mediated growth on Si(111) is a two step process which involves first incorporation of Si into a Sb(1 \times 1) domain [i.e., Si in the lower part and Sb in the upper part of the (111) bilayer].³ With further incorpora-

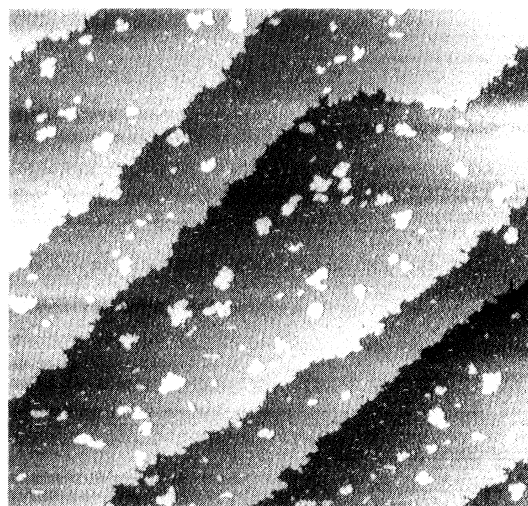


FIG. 4. Arsenic-mediated epitaxy of Si on Si(111) (3000×3000 Å, 530°C). Substrate step lines are running from the lower left to the upper right. Nucleation of irregular formed 2D islands with a high island density compared to pure Si homoepitaxy occurs.

tion of Si a complete Si bilayer forms with Sb trimers residing on top. This two step process is unlike the growth in pure Si/Si(111) epitaxy where a complete bilayer is formed directly.

As a second surfactant in Si/Si(111) homoepitaxy we used arsenic. On the (1×1) As covered surface one monolayer of As coverage is incorporated into the upper part of the Si(111) double layer.⁹ Figure 4 shows 0.1-ML Si evaporated onto the As covered Si(111) surface. Step lines running from the lower left to the upper right are visible. Nucleation of irregular islands on the terraces occurred. A quantitative analysis shows that also As as surfactant leads to an increased island density in Si/Si homoepitaxy. An Arrhenius behavior for the island density is found [Fig. 2(a)].

Ga AND In AS SURFACTANTS

A necessary condition to study the Si diffusion on a surfactant-covered surface is the preparation of large, flat terraces of the surfactant-covered starting surface. In the case of Ga and In as surfactant this turned out to be more difficult than for Sb and As, where saturation coverages were used. For Ga and In as surfactants we used the $\frac{1}{3}$ ML covered $(\sqrt{3}\times\sqrt{3})R30^\circ$ structures as starting surfaces, which are not saturation coverages.

Two different methods to prepare a $\frac{1}{3}$ ML $(\sqrt{3}\times\sqrt{3})R30^\circ$ Ga structure exist. First $\frac{1}{3}$ ML of Ga is evaporated at 400–500 °C (or evaporated and annealed afterwards).¹⁹ The second method is to evaporate first the saturation coverage of 1 ML of Ga and then anneal to 650 °C to evaporate excess Ga.^{13,20} While in both cases a clear $(\sqrt{3}\times\sqrt{3})R30^\circ$ LEED pattern is observed, only in the case where $\frac{1}{3}$ ML of Ga is evaporated, large flat terraces appear. When 1 ML of Ga is evaporated about one-half of the surface is covered by up to 2000-Å-large vacancy islands [Fig. 5(a)]. The occurrence of these vacancy islands when 1 ML of Ga is evaporated can be explained as follows: The Ga structure with 1 ML of Ga adsorbed is a (1×1) like structure,²⁰ 1 ML of Ga is incorporated into the upper part of the Si(111) double layer. During annealing and evaporation of excess Ga, 1 ML (= $\frac{1}{2}$ bilayer) silicon is transported over the surface to form a complete Si(111) bilayer (= 2 ML), which is covered by $\frac{1}{3}$ -ML Ga all over the surface [$(\sqrt{3}\times\sqrt{3})R30^\circ$ structure]. As a result of this mass transport process, which occurs over quite large distances (up to 1000 Å) the vacancy islands are formed. Only in the case where $\frac{1}{3}$ -ML Ga is evaporated from the beginning large flat terraces of $(\sqrt{3}\times\sqrt{3})R30^\circ$ structure occur which are necessary for our nucleation and diffusion experiments. Even on flat terraces the nucleation can be influenced by $(\sqrt{3}\times\sqrt{3})R30^\circ$ domain boundaries of the Ga structure. We observed that Si preferentially nucleates at these domain boundaries. Since we want to observe homogeneous nucleation in regions free from domain boundaries, we optimized the preparation in order to obtain large $(\sqrt{3}\times\sqrt{3})R30^\circ$ domain boundaries. The domain boundaries appear in large area STM scans as fine lines. We rejected images where nucleation at domain boundaries occurs. Figure 5(b) shows homogene-

ous nucleation of Si on a Ga $\sqrt{3}$ surface and denuded zones at the step edge. The scale ($2.1\times 1.6\ \mu\text{m}$) shows that the diffusion length of Si on the Ga-covered surface is much larger than for Sb or As. Si has about the same diffusion length on the Ga-covered surface as on the clean surface.

Finally, we used the In $(\sqrt{3}\times\sqrt{3})R30^\circ$ structure as surfactant layer. Here $\frac{1}{3}$ -ML In resides on top of a Si(111) bilayer.²¹ For In as surfactant the Si diffusion length turned out to be even larger than in pure Si epitaxy. To measure extremely large diffusion lengths, very wide Si terraces are required. Otherwise the wide denuded zones at both step edges terminating the terrace overlap and no nucleation of islands occurs. Since we had no highly oriented wafers available, we had to use the following *in situ* preparation to produce large terraces: Step bunching is observed when during dc heating (1200 °C) the current flows along step up direction.²² Between the step bunches (lower left in Fig. 6) wide terraces occur (middle of Fig. 6). Up to 1- μm -wide terraces can be pro-

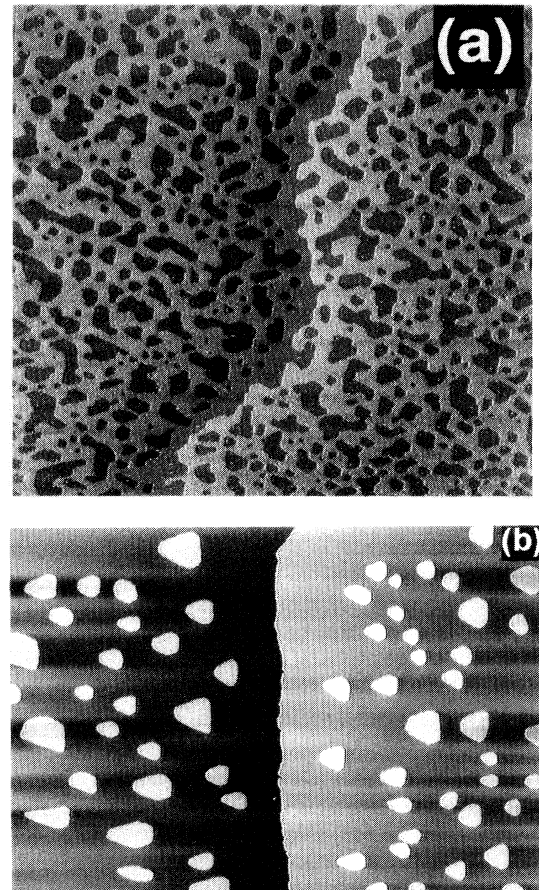


FIG. 5. (a) Ga $(\sqrt{3}\times\sqrt{3})R30^\circ$ surface with vacancies that occurred during transformation of the 1-ML Ga surface to the $(\sqrt{3}\times\sqrt{3})$ -Ga surface by evaporation of excess Ga. Mass transport of 1-ML Si leads to these vacancies. (b) Nucleation of 2D Si islands on the Ga $(\sqrt{3}\times\sqrt{3})$ terminated surface. A step edge runs in the middle of the image from the top to the bottom. Zones depleted from the island occur on both sides of the step edge ($2.1\times 1.6\ \mu\text{m}$, $T = 630^\circ$).

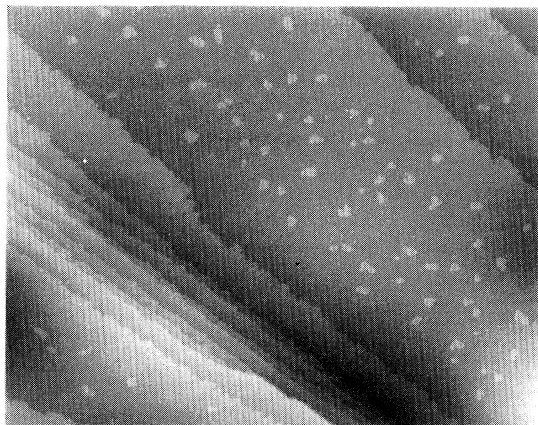


FIG. 6. Indium as surfactant in Si/Si(111) epitaxy ($8000 \times 6700 \text{ \AA}$). A step bunch is imaged in the lower left of the image. The large distance of several hundred \AA between the 2D Si islands at a low temperature of only 350°C shows the increased diffusivity of Si on the In covered surface.

duced with this method.

The In-terminated surfactant surface was prepared by evaporating $\frac{1}{3}$ -ML In at 580°C . Figure 6 shows silicon nucleation at 350°C on the In ($\sqrt{3} \times \sqrt{3}$) $R 30^\circ$ surface ($8000 \times 6700 \text{ \AA}$). Distances between the islands of several hundred angstroms already at this low temperature indicate very large diffusion distances for Si on the In covered surface. To observe homogeneous nucleation also at higher temperatures extremely wide terraces on the Si surface are required. If the terraces become too narrow the growth proceeds in the step flow growth mode. Arriving Si atoms diffuse to and are incorporated into the step edges. No nucleation occurs on narrow terraces (Fig. 6).

The Arrhenius plot [Fig. 2(a)] indicates how strong the diffusion is enhanced with In as surfactant. The island density in the In mediated epitaxy is 15 times lower than in pure Si/Si epitaxy at 400°C . The form of the islands is quite irregular which is unexpected for this large diffusion length. This means that in spite of the high rate of diffusion on the terraces the diffusion along the island edges is small. For diffusion along the island edges more bonds have to be broken than for diffusion on the free terraces. With In as a surfactant no preferred nucleation at the ($\sqrt{3} \times \sqrt{3}$) $R 30^\circ$ domain boundaries occurred.

GROWTH KINETICS IN SURFACTANT-MEDIATED Si/Si(111) EPITAXY

A priori two opposite models for the kinetics of Si adatoms on the surfactant-terminated surface are possible. First a model of easy diffusion is discussed. Diffusion of atoms arriving on the surfactant passivated surface can be rapid because all Si dangling bonds are saturated. Enhanced diffusion and incorporation below the surfactant layer at step edges leads to a step-flow growth mechanism. This model is supported by recent reflection electron microscopy experiments, which show enhanced

diffusion for surfactant-mediated growth of Si on Si(111).^{13,23} On the other hand, a model of hindered diffusion is possible. An arriving atom will not diffuse over large distances but the energetically favorable place exchange with a surfactant atom happens fast. Once incorporated below the surfactant layer, the diffusion is curtailed drastically. This model of reduced diffusion gives rise to an increased island density. Recent low-energy electron microscopy measurements for the system Ge/Si(100) with As as a surfactant²⁴ support this model. From a contrast fade away, it is concluded that 2D islands smaller than the resolution limit of the instrument ($\sim 150 \text{ \AA}$) are present on the surface.

This shows that surfactant-mediated epitaxy may lead to two opposing mechanisms of the growth kinetics, which give rise to layer growth. The study of the nucleation of 2D islands during submonolayer epitaxy by STM gives a quite direct access to the growth kinetics and can distinguish between different mechanisms in surfactant-mediated epitaxy.

During the course of our experiments, we analyzed the influence of four different surfactants on the growth kinetics of Si on Si(111). The results are summarized in Fig. 7, which shows the depleted zones (average between step-up and step-down depleted zones) as functions of $1/T$. As an operative definition of the diffusion length, we take the width of the depleted zones or the distance between the islands. This diffusion length is essentially only an effective diffusion length which is influenced by two factors: the generic diffusion length (determined by the energy barrier to hop from site to site) and the exchange process of the diffusing Si below the surfactant layer. Since this effective diffusion length is the main accessible experimental quantity describing the lateral distribution of nucleating Si on the surface, we will refer to it in the following as the diffusion length.

This diffusion length is drastically decreased for Sb and As as surfactants. This small effective diffusion length is a product of the two factors mentioned above. First the diffusion energy (the energy barrier to hop from site to site) can be higher on the surfactant covered surface than in pure Si/Si homoepitaxy. On the other hand, also, the site exchange process during surfactant-mediated epitaxy can reduce the effective diffusion length. The diffusivity to hop from site to site can be quite high, if, however, the energetically favorable site exchange process between the surfactant and the silicon occurs and silicon is incorporated below the surfactant layer, the diffusion is drastically curtailed. Once the Si is in the bulk position below the surfactant layer a quite high diffusion barrier has to be overcome to eject the Si on top of the surfactant layer for further diffusion. Also, this mechanism can lead to small effective diffusion length independent of the size of the diffusion barrier. It is difficult to separate these two factors influencing the effective diffusion length. We think that the exchange process is the dominant factor in reducing the diffusion length. If this exchange process would be a slow process, the experimentally observed floating of the surfactant layer could not be explained. Since the exchange process adds an unknown parameter, which is not modeled by the nucleation theory, we did

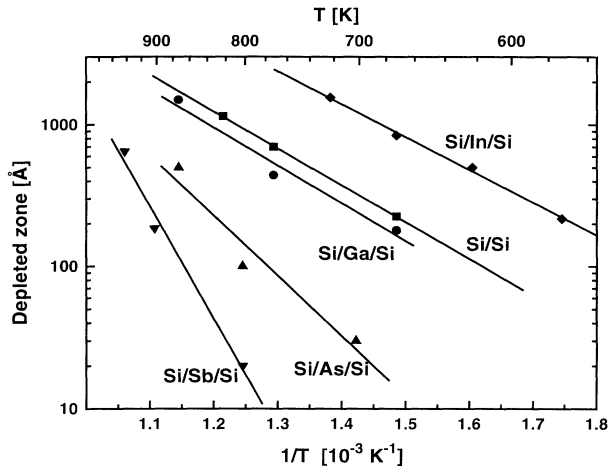


FIG. 7. Depleted zones at the step edges in Si/Si(111) epitaxy as function of the temperature. The width of the depleted zone is a measure of the diffusion length for Si adatoms. The depleted zone varies drastically in surfactant-mediated epitaxy. The depleted zone in In-mediated epitaxy is more than two orders of magnitude wider than the zone in Sb mediated epitaxy.

not apply classical nucleation theories to extract diffusion energies from these data.

Si atoms diffusing on the gallium surfactant layer have almost the same diffusion length as in the pure Si/Si epitaxy. Indium as surfactant induces a large Si diffusion length, which leads to wide depleted zones (Fig. 6). Like the other surfactants we studied, In is known to float up during Si growth.²⁵ Since an incorporation of diffusing Si atoms below the surfactant layer results in a reduction of the generic diffusion length the experimentally observed large diffusion length is due to a reduction of the diffusion energy for hopping from site to site.

Because the nucleation behavior is not governed by the incorporation process the classical nucleation theory used for Si/Si growth was also applied to the case where the diffusion is modified by indium. The data can be described by a critical nucleus size of three and a diffusion energy of 0.45 eV.

When we look at the shape of the nucleating 2D islands, we find that at a fixed temperature of 400°C for all surfactants used the shape is irregular, whereas the shape of 2D islands nucleating in pure Si/Si epitaxy is regular (triangular). In the case of Sb and As as surfactants the irregular shape can be explained by the reduced Si diffusion length. In the case of indium as surfactant, where increased diffusivity was observed on the terraces, the irregular island shapes can be explained by a reduced diffusion after the incorporation of the diffusing Si adatoms at the step edges, below the surfactant layer.

Since we performed all experiments at submonolayer silicon coverages the question arises how surfactants influence the growth kinetics of thicker layers and whether the drastically reduced diffusion length leads to a rough growth front for thicker films. We explored 5 ML

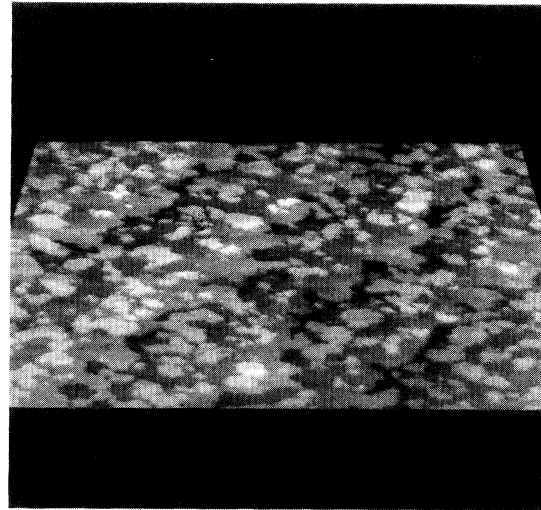


FIG. 8. Perspective view of 5 ML of Si grown at 600°C using Sb as surfactant ($3000 \times 3000 \text{ \AA}$). Step lines are running from the lower left to the upper right. In spite of the small diffusion distances the growth stays flat. Mainly one layer participates in the growth.

of Si grown with Sb as surfactant layer (600°C). In Fig. 8, four step lines are running from the upper right to the lower left of the image ($3000 \times 3000 \text{ \AA}$). These step lines have a rough appearance since some of the islands that nucleated on the terraces are connected to the step edges. A high island density on the terraces is also observed for this thicker layer. For pure Si epitaxy the depleted zone is $\approx 2000 \text{ \AA}$ at this temperature while the mean distance between the islands in Fig. 8 is $\approx 300 \text{ \AA}$. This small diffusion distance and high island density does not lead to a rough growth. Still after 5 ML there is mainly one layer growing on the terraces. This shows that the more local growth due to the reduced diffusion length does not preclude a flat growth.

The four surfactants studied here have a quite different influence on the growth kinetics during Si/Si(111) epitaxy. While Sb and As decrease the diffusion length and Ga leads to the same diffusion length as in Si homoepitaxy, In as surfactant increases the diffusivity of Si drastically. The depleted zone is almost three orders of magnitude larger for In than for Sb as surfactant ($T = 500^\circ\text{C}$) (Fig. 7). This large diffusion length in the In mediated epitaxy opens the possibility to grow Si in the desired step flow growth mode at much lower temperatures than in pure Si/Si epitaxy. In-mediated epitaxy would be a method to grow high-quality Si layers at extremely low temperatures. In the following the results gained in surfactant-mediated homoepitaxy are applied to the modification of heteroepitaxial growth of Ge on Si(111) by surfactants.

SURFACTANT-MEDIATED Ge/Si EPITAXY

One of the most tempting applications of growth modification by surfactants is the suppression of normally occurring 3D-island growth in Ge epitaxy on silicon.

Since Si and Ge are very similar elements, we will now carry over our results on the diffusion length in surfactant-mediated Si homoepitaxy to the Ge epitaxy on Si.

For the formation of large 3D Ge islands a mass transport over large distances is required. Typical distances between the Ge islands are several micrometers at temperatures above 400 °C. When we transfer the reduced Si diffusion length found for Sb as surfactant in Si homoepitaxy to the case of Ge/Si heteroepitaxy a reduced diffusion length is also expected here. This reduced diffusion of Ge hinders the mass transport of Ge, which is necessary for the formation of 3D islands. This kinetically limited growth is expected to suppress the 3D islands in Sb/Ge/Si(111) growth.

We tested this idea by increasing the diffusion in Sb mediated Ge epitaxy. Increasing the growth temperature increases the diffusion length above a certain limit, where formation of 3D islands occurs again.⁴ We believe that the reduction of the diffusion length is essential for the suppression of 3D islanding in Ge/Si heteroepitaxy. From our results we would predict that In, which promotes the diffusion of Si and Ge, does not suppress 3D islanding.

In Table I the available data on the diffusion length in surfactant-mediated Si/Si(111) epitaxy and on the promotion or suppression of 3D islanding in surfactant-mediated Ge/Si epitaxy are compiled.^{1,3,7,12,23,26-31} The ratio of the width of the depleted zone in surfactant-mediated epitaxy to the zone in pure Si homoepitaxy (g) is a quantity that describes the change in diffusion length due to surfactants. Values of $g > 1$ indicate increased and values of $g < 1$ reduced diffusion length, respectively, compared to the case of pure Si homoepitaxy. Elements of group III and IV (Ga, In, and Sn) as surfactants increase the Si diffusion length, while elements of group V (Sb,As) lead to a reduced Si diffusion length.

In the lower part of each element box is indicated in which cases 3D islanding in Ge epitaxy on Si occurs and for which surfactants 3D islanding can be suppressed in Ge/Si epitaxy. This table clearly indicates a correlation. The elements of group III and IV which induce high diffusion length in surfactant-mediated Si homoepitaxy do not suppress 3D islanding in Ge/Si epitaxy. For the elements of group V (and VI) which reduce the effective diffusion length, a suppression of 3D islanding is observed. Following Table I, we would predict that islanding occurs in In-mediated Ge/Si heteroepitaxy.

We can speculate on the reasons for the high diffusivity of Si for elements of group III and IV as surfactants and the reduced diffusion length for the elements of group V and VI as surfactants. For elements of group III as surfactants all three valence electrons participate in the bonds to the Si surface. The surface is completely passivated which may lead to a low barrier for hopping from site to site and hence to a high diffusivity of Si on these surfaces. Elements of group IV, V, and VI have one, two, and three valence electrons more, respectively. For instance, the elements of group V Sb and As have two valence electrons which protrude out of the surface as a lone pair orbital. With electrons sticking into the vacu-

TABLE I. Part of the Periodic Table of elements frequently used as surfactants in Si/Ge epitaxy. The value g defines the diffusion length in surfactant-mediated epitaxy relative to the pure Si/Si epitaxy. The diffusivity is increased for elements of group III and IV as surfactants and reduced for elements of group V and VI as surfactants. This behavior correlates with the tendency to suppress 3D islanding in Ge/Si epitaxy. Elements of group III and IV as surfactants do not suppress 3D islanding while elements of group V and VI, which reduce the diffusion length in Si/Si epitaxy suppress 3D islanding in heteroepitaxial growth of Ge on Si.

increased diffusion (Si/Si)		reduced diffusion (Si/Si)	
islanding (Ge/Si)		no islanding (Ge/Si)	
III	IV	V	VI
Ga g~5 ref. 12,31 g~1 this work islanding ref.26		As g~.05 this work no islanding ref.1	
In g~5 this work g>1 ref.25	Sn g>10 ref.23 islanding ref.27	Sb g~.025 this work no islanding ref.3	Te no islanding ref. 29,30
	Pb islanding ref.7	Bi no islanding ref.28	

um, these elements as surfactants may be more reactive to silicon and reduce the Si diffusion length this way.

In Ge/Si heteroepitaxy the reduced diffusion length suppresses mass transport over large distances, which is necessary for the formation of 3D islands. Also, in conventional epitaxy without surfactants, the diffusion length can be reduced by reducing the growth temperature. However, in this case with decreasing temperature, the formation of stacking fault defects degrades the epitaxial quality of the films. The stacking fault defects arise due to reduced bulk diffusion at low growth temperatures. Surfactant-mediated growth opens the possibility to selectively reduce the surface diffusion length without sacrificing the epitaxial quality of the grown film. The high growth temperature maintains a high bulk diffusion length that prevents formation of stacking fault defects. So it is possible to tune into the desired growth mode and simultaneously retain high epitaxial quality.

CONCLUSIONS

We have shown that different surfactants influence the kinetics in Si/Si epitaxy quite differently. Sb and As as surfactants reduce the diffusion distances of Si adatoms, while Ga as surfactant results in a similar Si diffusion on Si(111) like in pure Si/Si homoepitaxy, and In, on the other hand, increases the diffusivity of Si drastically.

When we apply these results to Ge/Si heteroepitaxy,

we see that the elements of group III and IV as surfactants (Ga,In,Sn,Pb), which promote diffusivity facilitate 3D islanding in Ge/Si heteroepitaxy and the elements of group V and VI (As,Sb,Bi,Te), which reduce the diffusion length suppress 3D islanding. Due to decreased diffusion length material transport over large distances which is necessary for 3D islanding is suppressed.

The diffusion energy and the critical nucleus size in Si/Si(111) epitaxy are determined in the framework of

classical nucleation theories. No indication for an Ehrlich-Schwoebel barrier for step-down diffusion of Si adatoms was found.

Note added in proof. From our results we predicted that indium-mediated Ge epitaxy should lead to 3D islanding of Ge due to the large diffusion length measured in indium-mediated epitaxy. Indeed, recently Minoda *et al.* found 3D islanding of Ge in indium-mediated epitaxy.³²

-
- ¹M. Copel, M. C. Reuter, E. Kaxiras, and R. M. Tromp, *Phys. Rev. Lett.* **63**, 632 (1989).
- ²M. Horn-von Hoegen, F. K. LeGoues, M. Copel, M. C. Reuter, and R. M. Tromp, *Phys. Rev. Lett.* **67**, 1130 (1991).
- ³G. Meyer, B. Voigtländer, and N. M. Amer, *Surf. Sci.* **272**, L541 (1992).
- ⁴B. Voigtländer and A. Zinner, *J. Vac. Sci. Technol. A* **12**, 1932 (1994).
- ⁵U. Menczigar, G. Abstreiter, J. Olajos, H. Grimmeiss, H. Kibbel, H. Presting, and E. Kasper, *Phys. Rev. B* **47**, 4099 (1993).
- ⁶H. Presting, U. Menczigar, and H. Kibbel, *J. Vac. Sci. Technol. B* **11**, 1110 (1993).
- ⁷H. Hibino, N. Shimizu, K. Sumitomo, Y. Shinoda, T. Nishio-ka, and T. Ogino, *J. Vac. Sci. Technol. A* **12**, 23 (1994).
- ⁸B. Voigtländer and A. Zinner, *Surf. Sci.* **292**, L775 (1993).
- ⁹J. R. Patel, J. A. Golovchenko, P. E. Freeland, and H-J. Gossmann, *Phys. Rev. B* **36**, 7715 (1987).
- ¹⁰Y.-W. Mo, J. Kleiner, M. B. Webb, and M. G. Lagally, *Surf. Sci.* **268**, 275 (1992).
- ¹¹J. A. Venables, G. D. T. Spiller, and M. Hanbücken, *Rep. Prog. Phys.* **47**, 399 (1984).
- ¹²U. Köhler, J. E. Demuth, and R. J. Hamers, *J. Vac. Sci. Technol. A* **7**, 2860 (1989).
- ¹³H. Nakahara and M. Ichikawa, *Appl. Phys. Lett.* **61**, 1531 (1992).
- ¹⁴R. E. Honig, and D. A. Kramer, *RCA Rev.* **30**, 285 (1969).
- ¹⁵J. Tersoff, A. W. Denier van der Gon, and R. M. Tromp, *Phys. Rev. Lett.* **72**, 226 (1994).
- ¹⁶H. A. Van der Vegt, H. M. van der Pinxteren, M. Lohmeyer, E. Vlieg, and J. M. C. Thornton, *Phys. Rev. Lett.* **68**, 3335 (1992).
- ¹⁷S. C. Wang and G. Ehrlich, *Phys. Rev. Lett.* **67**, 2509 (1991).
- ¹⁸P. Mårtensson, G. Meyer, N. M. Amer, E. Kaxiras, and K. C. Pandey, *Phys. Rev. B* **42**, 7230 (1990).
- ¹⁹J. Nogami, Sang-il Park, and C. F. Quate, *Surf. Sci.* **203**, L631 (1988).
- ²⁰J. Zegenhagen, M. S. Hybertsen, P. E. Freeland, and J. R. Patel, *Phys. Rev. B* **38**, 7885 (1988).
- ²¹J. Nogami, Sang-il Park, and C. F. Quate, *Phys. Rev. B* **36**, 6221 (1987).
- ²²H. Tokumoto, K. Miki, H. Murakami, and K. Kajimura, *J. Vac. Sci. Technol. B* **9**, 699 (1991).
- ²³S. Iwanari and K. Takayanagi, *Jpn. J. Appl. Phys.* **30**, L1978 (1991).
- ²⁴R. M. Tromp and M. C. Reuter, *Phys. Rev. Lett.* **68**, 954 (1992).
- ²⁵H. Minoda, Y. Tanishiro, N. Yamamoto, and K. Yagi, *Surf. Sci.* **278/288**, 915 (1993).
- ²⁶J. Falta, M. Copel, F. K. LeGouess, and R. M. Tromp, *Appl. Phys. Lett.* **62**, 2962 (1993).
- ²⁷W. Dondl, G. Lütering, W. Wegscheider, J. Wilhelm, R. Schorer, and G. Abstreiter, *J. Cryst. Growth* **127**, 440 (1993).
- ²⁸A. Kawano, I. Konomi, H. Azuma, T. Hioki, and S. Noda, *J. Appl. Phys.* **74**, 4265 (1993).
- ²⁹S. Higuchi and Y. Nakanishi, *Surf. Sci.* **254**, L465 (1991).
- ³⁰H. J. Osten, J. Klatt, G. Lippert, E. Bugiel, and S. Higuchi, *J. Appl. Phys.* **74**, 2507 (1993).
- ³¹H. Nakahara and M. Ichikawa, *Surf. Sci.* **298**, 440 (1993).
- ³²H. Minoda and K. Yagi, *Surf. Rev. Lett.* **2** (1) (1995).

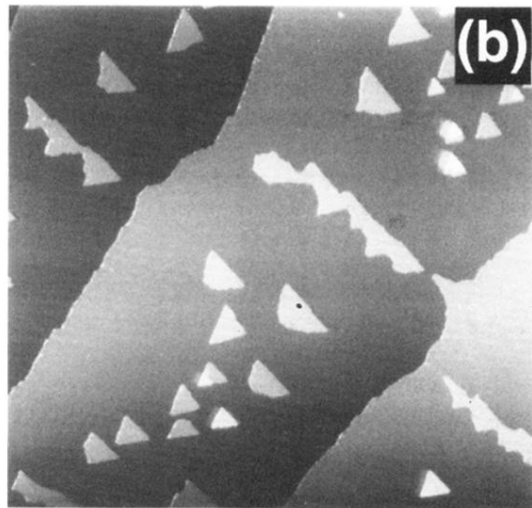
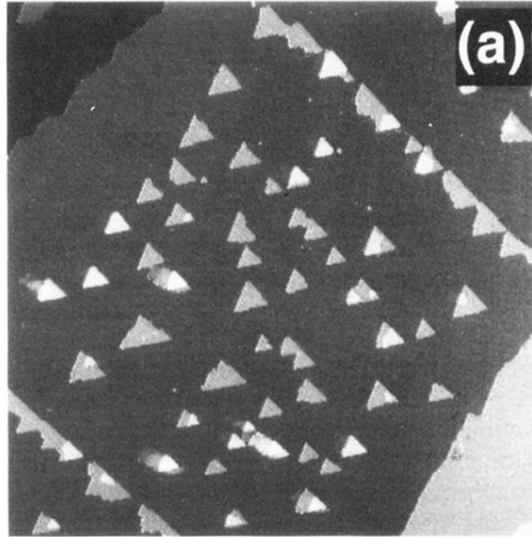


FIG. 1. Scanning-tunneling-microscopy images of 2D Si islands on a Si(111) terrace. Preferred nucleation occurs at (7×7) domain boundaries and depleted zones exist near step edges. (a) Area: $5800 \times 5800 \text{ \AA}$, $T = 500^\circ\text{C}$. (b) Epitaxy at higher temperature results in wider depleted zones and smaller island densities (area: $9100 \times 8600 \text{ \AA}$, $T = 550^\circ\text{C}$).

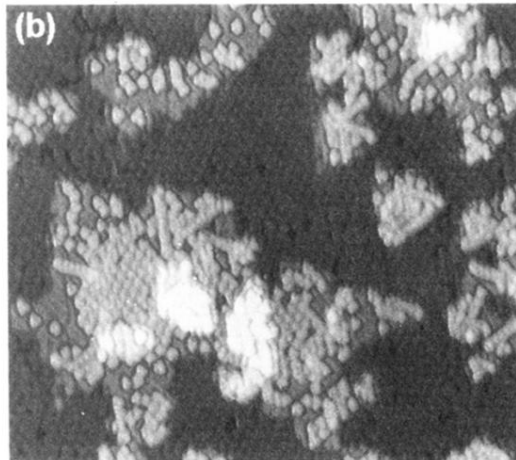
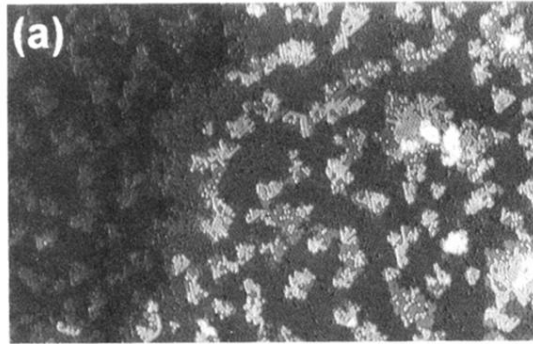


FIG. 3. Antimony-mediated epitaxy of Si on Si(111) ($T = 530^\circ\text{C}$) increases the island density drastically and reduces diffusion length. (a) Area: $975 \times 620 \text{ \AA}$; (b) higher-resolution scan of upper right in (a), area: $325 \times 290 \text{ \AA}$. The surface is completely covered by Sb. On the silicon terrace and on top of the 2D islands a $(\sqrt{3} \times \sqrt{3})$ -Sb structure is observed. The flat areas at the edges of the islands are Sb(1×1).

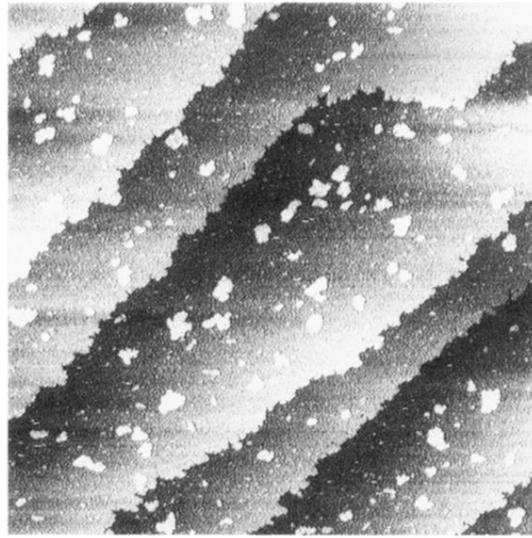


FIG. 4. Arsenic-mediated epitaxy of Si on Si(111) ($3000 \times 3000 \text{ \AA}$, 530°C). Substrate step lines are running from the lower left to the upper right. Nucleation of irregular formed 2D islands with a high island density compared to pure Si homoepitaxy occurs.

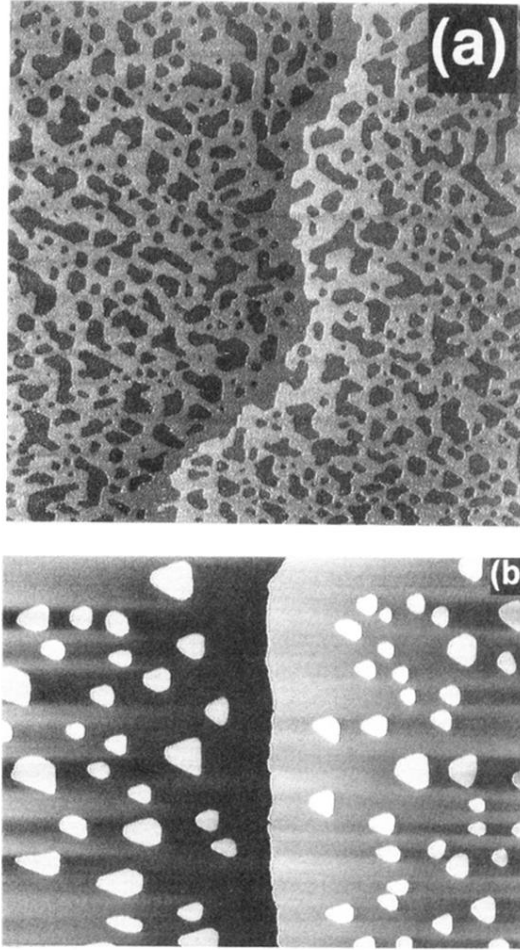


FIG. 5. (a) Ga $(\sqrt{3} \times \sqrt{3})R30^\circ$ surface with vacancies that occurred during transformation of the 1-ML Ga surface to the $(\sqrt{3} \times \sqrt{3})$ -Ga surface by evaporation of excess Ga. Mass transport of 1-ML Si leads to these vacancies. (b) Nucleation of 2D Si islands on the Ga $(\sqrt{3} \times \sqrt{3})$ terminated surface. A step edge runs in the middle of the image from the top to the bottom. Zones depleted from the island occur on both sides of the step edge ($2.1 \times 1.6 \mu\text{m}$, $T = 630^\circ$).

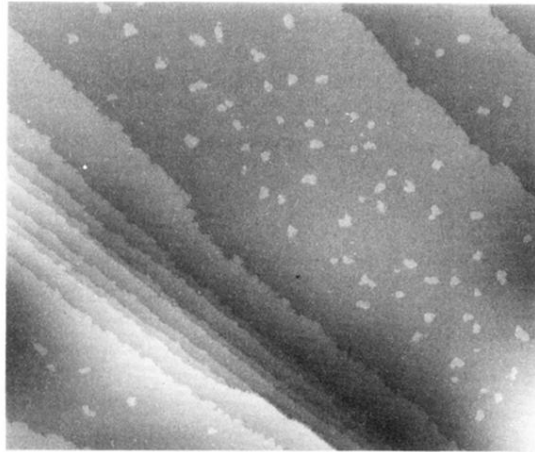


FIG. 6. Indium as surfactant in Si/Si(111) epitaxy ($8000 \times 6700 \text{ \AA}$). A step bunch is imaged in the lower left of the image. The large distance of several hundred \AA between the 2D Si islands at a low temperature of only 350°C shows the increased diffusivity of Si on the In covered surface.

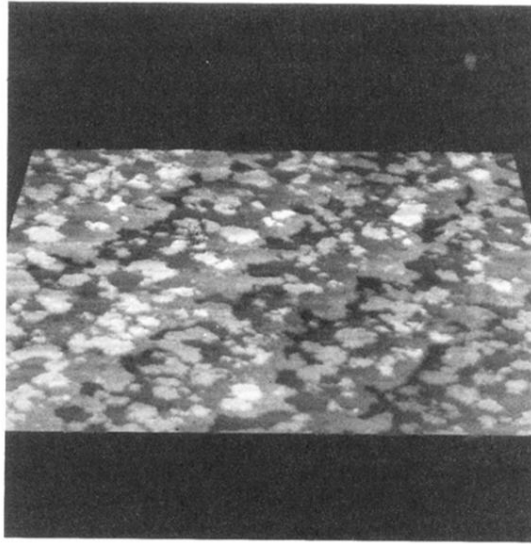


FIG. 8. Perspective view of 5 ML of Si grown at 600 °C using Sb as surfactant ($3000 \times 3000 \text{ \AA}$). Step lines are running from the lower left to the upper right. In spite of the small diffusion distances the growth stays flat. Mainly one layer participates in the growth.